Am J Transl Res 2021;13(11):12364-12374
www.ajtr.org /ISSN:1943-8141/AJTR0135348

Original Article

The perioral muscle continuum affects premaxillary development in Wistar rats

Feng Yang[1*], Weiwei Bian[1*], Rao Fu[1*], Jing Wang[2], Jian Wang[1], Jia Zhou[1]

[1]Department of Plastic and Reconstructive Surgery, Shanghai Ninth People's Hospital, Shanghai Jiao Tong University, School of Medicine, No. 639 Zhizaoju Road, Shanghai 200011, China; [2]Department of Otorhinolaryngology Head and Neck Surgery, Shanghai Children's Hospital, Shanghai Jiao Tong University, 355 Luding Road, Shanghai 200011, China. [*]Equal contributors and co-first authors.

Received May 17, 2021; Accepted August 24, 2021; Epub November 15, 2021; Published November 30, 2021

Abstract: Craniofacial deformities involve soft tissue and skeletal abnormalities. Facial bone growth is based on congenital defects and iatrogenic factors, in which muscle activity is important. Understanding the effects of muscle function on facial bone growth may help us in clinical treatment. Although there have been some studies, fewer have focused on the effects of perioral muscle continuity on maxillary development, which needs further research. In our study, mimic perioral muscle surgeries were performed in twenty 3-day Wistar rats, which were divided into four equal groups, including five untreated rats as control (Ctrl), five rats by unilateral perioral muscle incision (MI), five rats by unilateral perioral muscle incision combined with muscle stripping (MIMS) and five rats treated by unilateral perioral muscle incision combined with periosteal stripping (MIPS). After six weeks, skulls were imaged and measured by micro-CT scan and hematoxylin-eosin staining. Differences in the rats' premaxilla were analyzed with self-contrasted and group-control studies. Compared with Ctrl group, there were significant premaxillary developmental defects in the affected side of the rats in all three surgical groups. In the affected side, both the width and the length of the premaxilla were less than the unaffected side, particularly in MIMS and MIPS groups. Group-control study showed that the ratio of premaxillary length of affected side to unaffected side had significant differences between MI and MIMS. The conclusion was that complete perioral muscle continuity with intact muscle attachment on the premaxilla is the driving force for the premaxillary development.

Keywords: Craniofacial deformity, premaxilla, bone development, facial asymmetry, perioral musculature, cephalometry

Introduction

Approximately 60 muscles make up the craniofacial skeletal muscle completing the function of food uptake, eye movement and facial expression [1]. The shape of the craniofacial skeleton is constantly changing through ontogeny and reflects a balance between development patterning and mechanical-load-induced remodeling [2]. Muscles are a major contributor to produce the mechanical environment that is crucial for normal skull development [3]. Some studies reflected the relationship between craniofacial muscle and bone development. Kana Kono et al. [4] explored the influence between masticatory force and craniofacial development through building two groups of mice fed a powdered soft diet or conventional hard diet, and found reduced 3D bony development at the region where the chewing muscles attach, and an anterior shift in the temporal and parietal bone regions in soft diet group. Conith et al. [5] confirmed muscle-induced loading is an important source of variation in craniofacial skeletal shape by using an F5 hybrid population of Lake Malawi cichlids and identified three types of associations between muscles and bone: weak, strong direct and strong indirect. As for some clinical studies, masticatory muscles influence craniofacial growth in young individuals. Pepicelli et al. [6] concluded people with strong or thick mandibular muscles have wider transverse craniofacial dimensions and a tendency towards transverse parallelism between the jaw bases and between the occlusal and mandibular planes. All those studies used different methods to observe the muscle effects on skeletal development by altering

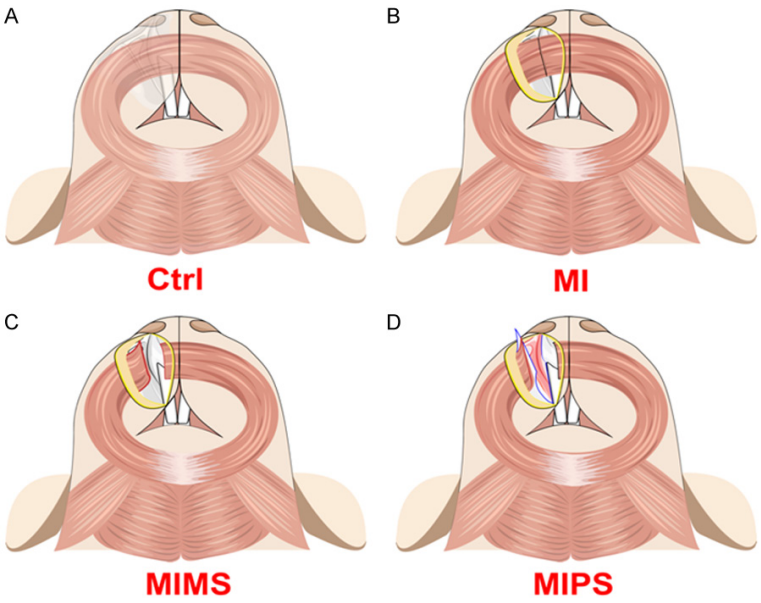

Figure 1. The mimic surgical schematic diagram of each group. (A) Control group: no surgery, (B) Muscle incision group, (C) Muscle incision combined with muscle stripping, (D) Muscle incision combined with periosteal stripping.

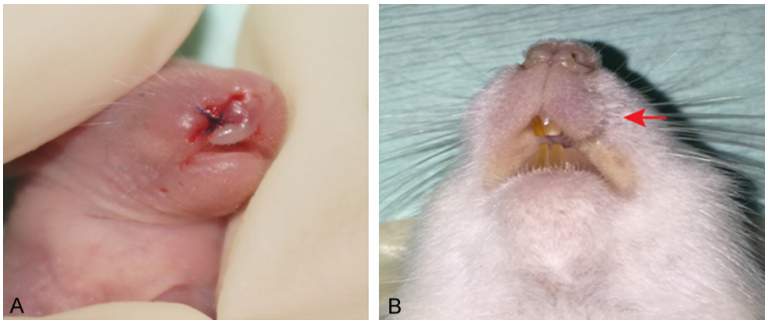

Figure 2. (A) Image of experimental newborn rat immediately post-surgery, (B) The surgical scar noted by the red arrow can be clearly identified at six weeks after the surgery.

muscle stretch but preserved muscle continuum and integrity. However, clinical craniofacial deformities, especially cleft lip and palate have defects of both facial muscle and bone development. Unfortunately, most prior studies have been limited, not addressing the impact of muscle integrity.

A study has reported that skeletal muscle stretch can regulate the growth of its attaching bone [7]. Whether the break-in perioral muscle continuity may impair maxillary growth has not been studied. To eliminate the superimposed effects of surgery and clarify the effects of perioral muscle continuity on craniofacial development, we provided a novel experimental idea. We found that complete perioral muscle continuity with intact muscle attachment on the premaxilla was the driving force for premaxillary development in rats.

Materials and methods

Animals and surgical procedures

20 newborn 3-day rats (provided by Shanghai SLAC Laboratory Animal Co. Ltd, Shanghai, China) were randomly divided into four groups on average: control group without treatment (Ctrl), unilateral perioral muscle incision group (MI), unilateral perioral muscle incision combined with muscle stripping group (MIMS), and unilateral perioral muscle incision combined with periosteal stripping group (MIPS). The surgical methods were elaborated as follows: one random side of the upper lip was cut full-thickness from the nostril to the lip margin. The rats in MI group only underwent the incision of skin, perioral muscle and mucosa. In MIMS group, the perioral musculature was bluntly dissected from its attachments to the premaxilla through the superficial periosteal layer, keeping the periosteum intact. In MIPS group, the plane of dissection was sub-periosteal (**Figure 1**). The wounds of both sides were sutured from mucosa to skin separately, to prevent the incision from re-adhesion (**Figure 2**). All procedures were performed by a single surgeon (J.Z.). During the next six weeks, no significant impact was observed on feeding and chewing in all groups. All of the experimental procedures were approved by the Committees of Animal Ethics and Experimental Safety of Shanghai Ninth People's Hospital.

MicroCT analysis and 3D reconstruction

The skulls of experimental rats were harvested at six weeks post-op. The harvested skulls

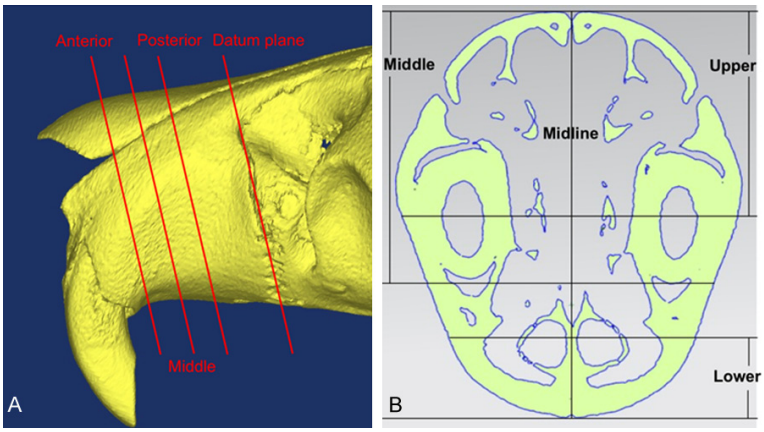

Figure 3. Methods of distance measurement in 2D coronal section. A. A coronal screenshot was taken parallel to the datum plane in three different lengths-anterior (one-third), middle (one-half) and posterior (two-thirds) respectively. B. The distance from the premaxillary margin to midline in three different premaxillary heights-upper (one-half), middle (two-thirds) and lower (four-fifths) respectively. Width of premaxilla was measured in 2D coronal cross-section of three different positions-the first anterior third level, the middle half level, and the last posterior third level respectively.

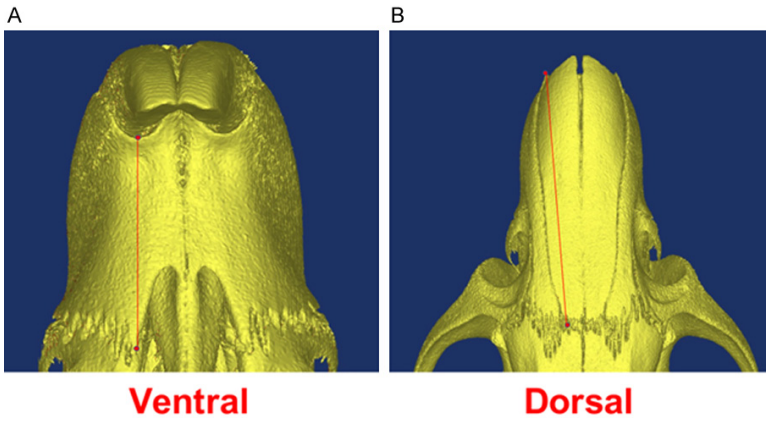

Figure 4. The pictures represent the cephalometric length measurement method of rat premaxilla on ventral view (A) and on dorsal view (B). On the ventral view, the premaxillary length was the distance from the posterior edge of the incisor groove to the inside of the suture (the premaxillary and maxillary suture), and on the dorsal view it was the distance from the most distal part of the premaxilla to the intersection of the premaxilla, nasal bone, and frontal bone on the sutura transversalis.

were fixed in 4% paraformaldehyde for 2 days prior to MicroCT scanning by the same operator (Shanghai Hongxin Technology Biological Co. Ltd, PerkinElmer Co. Ltd). The settings of the CT scanner were as follows: 90 KV voltage for the X-ray tube, 88 μA current for the X-ray source and 14 minutes of exposure time. The detector and the X-ray source were in a sagittal median axis and a 360-degree annular mode. The preset pattern was high resolution and the stage control was 70 mm. The original data was imported into Mimics 19.0 (Materialise, Mimics Research, 18.0 x64. Ink) for 3D reconstruction, and the predefined threshold of default maker was set to 700-Max to calculate the 3D value.

Cephalometric measurement

Cephalometric points were identified and measurements were performed to evaluate the premaxillary growth in microCT reconstructed 3D images on both the affected and unaffected sides. Sample cephalometric width measurement points are shown and described in **Figure 3**. Premaxillary sagittal length measurements are identified as follows, **Figure 4**: For the ventral view, the distances from posterior edge of the incisor groove to the inside of the suture (the premaxillary and maxillary suture) were measured on both affected and unaffected sides. For the dorsal view, the distances from the most distal part of the premaxilla to the intersection of the premaxilla, nasal bone, and frontal bone on the sutura transversalis were measured both on the affected and unaffected sides. The model for these measurements was based on previously published animal experiments [8, 9] and clinical anthropometric points by X-ray [10-12].

The reconstructed 3D images were imported into UG NX 11.0 reverse engineering software in SLT format. The plane formed by the bony suture between the premaxilla and maxilla was the datum plane. A coronal screenshot was taken parallel to the datum plane, and 2D cross-sections were used to view the linear contour of the fault. It was assumed that an abnormal area would occur in the middle of the premaxilla. We, therefore, halved the premaxilla in sagittal position and used the projection of

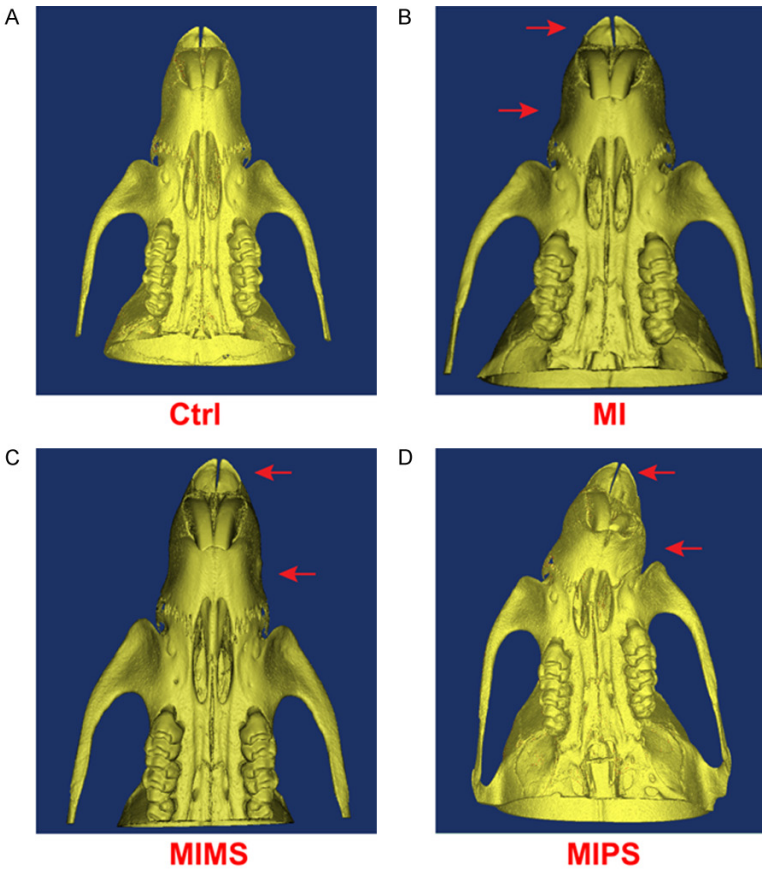

Figure 5. Micro-CT three-dimensional reconstruction images of the premaxilla. A. Ctrl group: Bilateral symmetry. B. MI group: the nasal bone was offset to the affected side. C. MIMS group: Significant defect in the premaxilla represented on the affected side, and the nasal bone was shifted to the affected side. D. MIPS group: severe destruction of the affected premaxilla. Red arrows indicate the affected side.

bisecting plane on 2D cross-sections as the midline. Coronal 2D cross-sections of the premaxilla were extracted in three different premaxillary lengths-anterior (one-third), middle (one-half) and posterior (two-thirds) respectively. Given the presence of the nasal bone in the coronal position, we selected three premaxillary heights-upper (one-half), middle (two-thirds) and lower (four-fifths) in the sectional views by Photoshop (**Figure 3**). The actual distance was equal to the ratio of the measured distance to the total rate of two magnifications when in the reverse engineering software and Photoshop.

Histologic examination

After the decapitation, the skulls were taken and fixed with 4% paraformaldehyde for 24 hours and preliminarily decalcified by 12.5% ethylenediaminetetraacetic acid for a month. The skulls were then trimmed intensively and sufficiently decalcified by 12.5% ethylenediaminetetraacetic acid for a month. Samples were washed multiple times with water before being embedded in paraffin, cut into 5-μm sections, mounted on slides, and deparaffinized by baking at 55 to 60°C. The slides were stained with hematoxylin and eosin, scanned using a Panoramic MIDI 3D digital slice scanning system and examined under a Case Viewer digital microscope. Devices were provided by 3D HISTECH Co. Ltd.

Statistical analysis

Results were reported as the mean ± s.d. of at least three independent experiments. A paired T-test was used to determine significance between two groups. A *P*-value of less than 0.05 was considered significant. SPSS 20.0 (SPSS Inc., Chicago, IL, USA) was used for the statistical analyses.

Results

3D imaging and coronal section analysis of rats

We compared 3D images of the skulls between the four groups. In the Ctrl group, the skulls showed good symmetry on both sides of the premaxilla, and the temporomandibular joints were normal without deviation. In contrast, in the MIPS group, the skulls showed the most severe periosteal destruction with impaired bony development in the premaxillary area and deviation of the front end of the nasal bone towards the affected side. In the MIMS group, bony depression on the surgical premaxillary side was also identified. Compared with the MIPS and MIMS groups, the premaxilla of the affected side was slightly depressed in the MI group, and the nasal offset was not as obvious (**Figure 5**). On cross-sectional imaging, bony

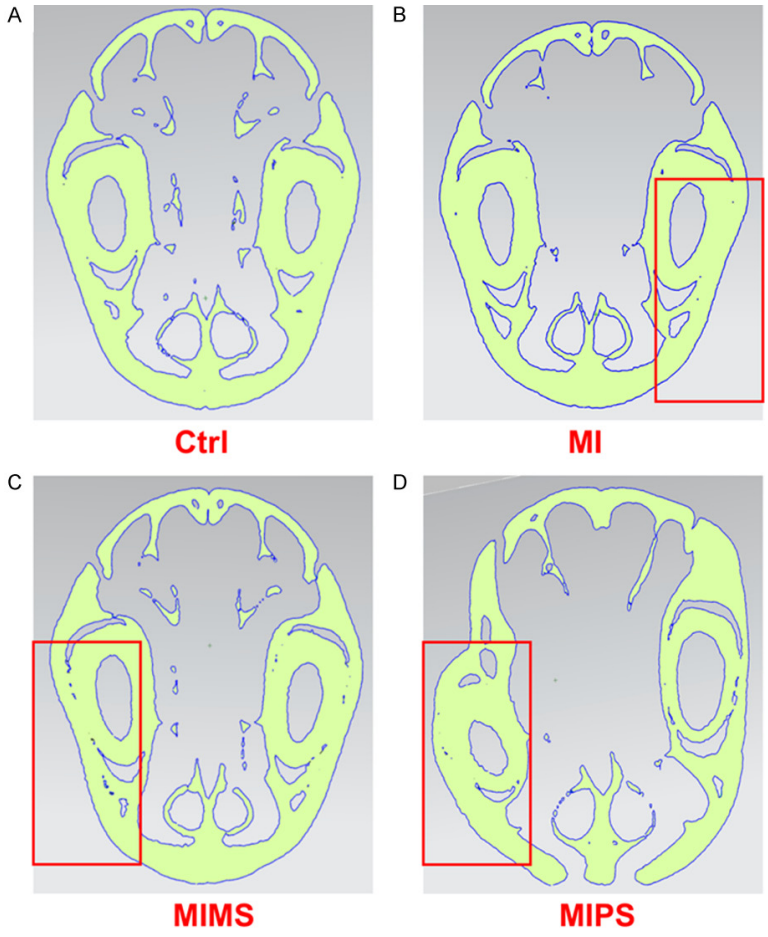

Figure 6. 2-D coronal cross-section images of the premaxilla in the middle half level. A. Ctrl group: Bilateral symmetry; B and C. MI and MIMS group: two sides of premaxilla are asymmetrical, and photographs show maldevelopment of premaxilla on the affected side; D. Serious deformation of the affected side premaxilla was observed in the MIPS group. Red rectangles indicate the affected side of the premaxilla.

depression on the surgical premaxillary side can be clearly observed in all three experimental groups with the most severe depression occurring in the MIPS group as expected (**Figure 6**).

Analysis results of cephalometric measurements

To quantify the gross visual results, we performed cephalometric measurements of the distance from each surface to the median line at different heights of different cross-sections using Photoshop (**Figure 3**). There was no difference between the two sides in the Ctrl group in both the sagittal and horizontal sections. In the sagittal section, premaxillary width measurements of the affected sides at three different heights including upper (one-half), middle (two-thirds) and lower (four-fifths) were not statistically different in the MI group ($P>0.05$), although the data showed that the average value of distance from the edge to the midline was wider than on the unaffected side. A significant difference was seen between the two sides in the MIMS group. At the anterior (one-third) length of the entire premaxillary bone, three different height measurements showed that the affected side was shorter than the unaffected side, but only the measurement of middle (two-thirds) was statistically different ($P=0.0040$). When middle (one-half) premaxillary length was measured, there was a significant difference at upper (one-half) ($P=0.002$) and the middle (two thirds) height ($P=0.001$). At the posterior (two thirds) length, only the upper (two-thirds) premaxillary height had a statistically significant difference ($P=0.030$) (**Figure 7**; **Table 1**). Due to the severe offset of the midline, we did not measure these data in MIPS. However, obvious developmental damage on the affected side could be observed on 3D images.

Premaxillary length measurements also showed some differences. Ventrally, most measurements of the affected side were significantly less than the measurements of the unaffected side in all three surgical groups, for MI ($P=0.034$), MIMS ($P=0.01$) and MIPS ($P=0.038$) groups. Dorsally, measurements of the affected side were significantly shorter than the measurements of the unaffected side in the MIPS group ($P=0.044$) (**Figure 7**; **Table 2**).

The ratio of measurements in affected sides to unaffected sides was used for the comparison between each pair of groups. Compared with the blank Ctrl group, significant differences

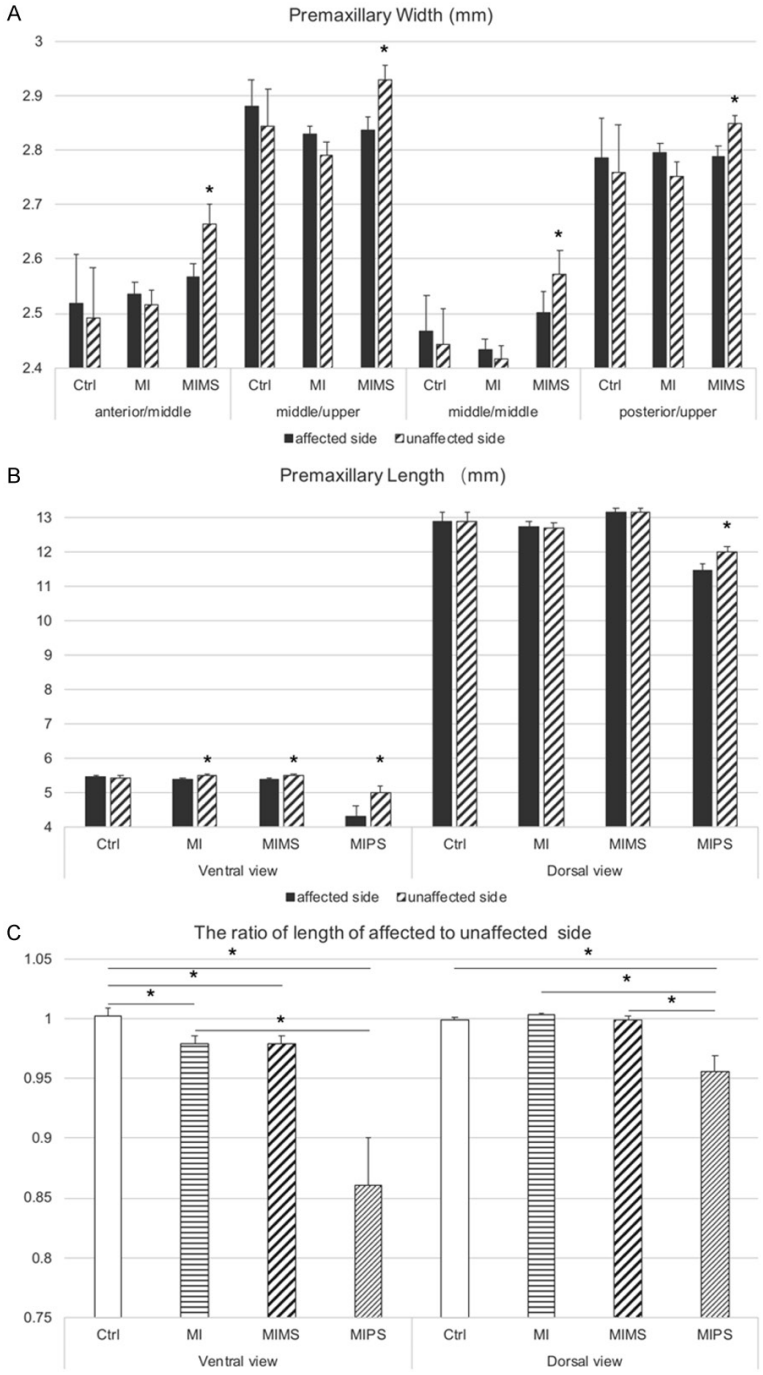

Figure 7. A. The histogram demonstrates significant differences between the premaxillary widths of two sides by self-contrasted study in four of the nine positions. They were anterior/middle, middle/upper, middle/middle and posterior/upper. B. On the ventral view, the lengths of premaxilla were significantly different between affected and unaffected sides in MI, MIMS, and MIPS groups. On dorsal view, there were significant differences in lengths of premaxilla between two sides only in the MIPS group. C. In the group-control study about the ratio of premaxillary length of the affected to unaffected side, the histogram shows significant differences between the MIPS and other groups. On the ventral view, the lengths were significantly different between the MIMS and Ctrl group. $^{*}P<0.05$.

were present in all three experimental groups, indicating that the premaxillary length was shorter than in the Ctrl group. There was no difference when the MI and MIMS groups were compared. When these two groups were compared with the MIPS group, results showed the ratios of dorsal view in both MI group (P=0.033) and MIMS group (P=0.037) were longer (**Figure 7**; **Table 3**).

Results of H&E staining

Hematoxylin and eosin staining was performed to assess whether the micro-computed tomographic results were consistent with histologic appearance. Our results showed a difference in the amount of premaxillary bone between Ctrl and the other three groups. In the Ctrl group, H&E staining showed that muscles were entirely attached to both sides of the premaxillary bone. The MIPS group showed severe bony destruction at the surgical site corresponding to the location of muscle and periosteal division. In the MI group, in which muscle continuity was interrupted without damage to the muscle attachment points, there was no difference between the two sides of premaxillary bone. In the MIMS group, the periosteum was continuous and intact on both sides, and the muscle was shredded after being decalcified (**Figure 8**).

Discussion

Previous studies have proven that facial muscle, especially muscle contractions, play a central role in bone growth [13, 14]. Effects of muscle

Table 1. Statistical data comparison of premaxillary width between affected and unaffected sides in Ctrl, MI, and MIMS groups

Location	Ctrl (n=5)	MI (n=5)	MIMS (n=5)
	Mean difference (SD, P)	Mean difference (SD, P)	Mean difference (SD, P)
Anterior			
Upper	0.036 (0.027, 0.071)	0.053 (0.064, 0.135)	-0.079 (0.111, 0.064)
Middle height	0.027 (0.037, 0.245)	0.021 (0.030, 0.196)	-0.097 (0.074, 0.004)*
Lower	0.024 (0.050, 0.413)	0.022 (0.070,0.532)	-0.030 (0.067, 0.214)
Middle			
Upper	0.036 (0.047, 0.224)	0.040 (0.035, 0.064)	-0.092 (0.062, 0.002)*
Middle height	0.023 (0.027, 0.179)	0.018 (0.045, 0.426)	-0.071 (0.043, 0.001)*
Lower	0.034 (0.051, 0.273)	0.024 (0.057, 0.404)	0.012 (0.062, 0.589)
Posterior			
Upper	0.027 (0.031, 0.180)	0.043 (0.0440, 0.094)	-0.060 (0.069, 0.030)*
Middle height	0.021 (0.025, 0.196)	0.050 (0.060, 0.139)	-0.036 (0.059, 0.105)
Lower	0.019 (0.018, 0.120)	0.012 (0.063, 0.697)	0.008 (0.048, 0.651)

Note: *$P<0.05$.

Table 2. Statistical data comparison of premaxillary length between affected and unaffected sides in all groups

Location	Ctrl (n=5)	MI (n=5)	MIMS (n=5)	MIPS (n=5)
	Mean (SD, P)	Mean (SD, P)	Mean (SD, P)	Mean (SD, P)
Ventral view	0.013 (0.071, 0.749)	-0.114 (0.080, 0.034)*	-0.114 (0.103, 0.010)*	-0.688 (0.193, 0.038)*
Dorsal view	-0.010 (0.045, 0.690)	0.046 (0.037, 0.050)	-0.011 (0.148, 0.827)	-0.525 (0.313, 0.044)*

Note: *$P<0.05$.

Table 3. Statistical data comparison of the ratio of maxillary length on the affected side to the unaffected side between each group

Comparison	Mean ± SD	Mean ± SD	T	*P*-value
MIPS vs Ctrl	MIPS	Ctrl		
Ventral view	0.861±0.080	1.002±0.013	-3.504	0.013*
Dorsal view	0.956±0.025	0.999±0.004	-3.357	0.041*
MI vs Ctrl	MI	Ctrl		
Ventral view	0.979±0.014	1.002±0.013	-2.457	0.044*
Dorsal view	1.004±0.003	0.999±0.004	2.103	0.074
MIMS vs Ctrl	MIMS	Ctrl		
Ventral view	0.979±0.019	1.002±0.013	-2.209	0.049*
Dorsal view	0.999±0.011	0.999±0.004	0.016	0.988
MIPS vs MI	MIPS	MI		
Ventral view	0.861±0.080	0.979±0.014	-3.315	0.013*
Dorsal view	0.956±0.025	1.004±0.003	-3.725	0.033*
MIMS vs MI	MIMS	MI		
Ventral view	0.979±0.019	0.980±0.014	-0.028	0.978
Dorsal view	0.999±0.011	1.004±0.003	-1.112	0.293
MIPS vs MIMS	MIPS	MI		
Ventral view	0.861±0.080	0.979±0.019	-2.931	0.057
Dorsal view	0.956±0.025	0.999±0.011	-3.255	0.037*

Note: *$P<0.05$.

atrophy on bone development have also been reported. Common experimental methods include changing the chewing method by soft diet feeding, drug injection to reduce muscle contraction, and myectomy or denervation. Seok et al. [5] induced masseter muscle paralysis with botulinum toxin A (BTX-A) injection and observed a growth decrease in the mandible. Matic et al. [8] also saw a significant decrease in volumes with minimal changes in shape and bone production decline by SPECT on the paralyzed side. Bresin et al. [15] demonstrated that feeding rats a soft diet could decrease bone mass and density in mandibular alveolar bone and thus considered that the function of the masticatory muscle was a determinant of the amount and density of cortical and trabecular bone. Furthermore, it was found by Katsaros et al. [16] that changes in masticatory muscle function also affected the transverse

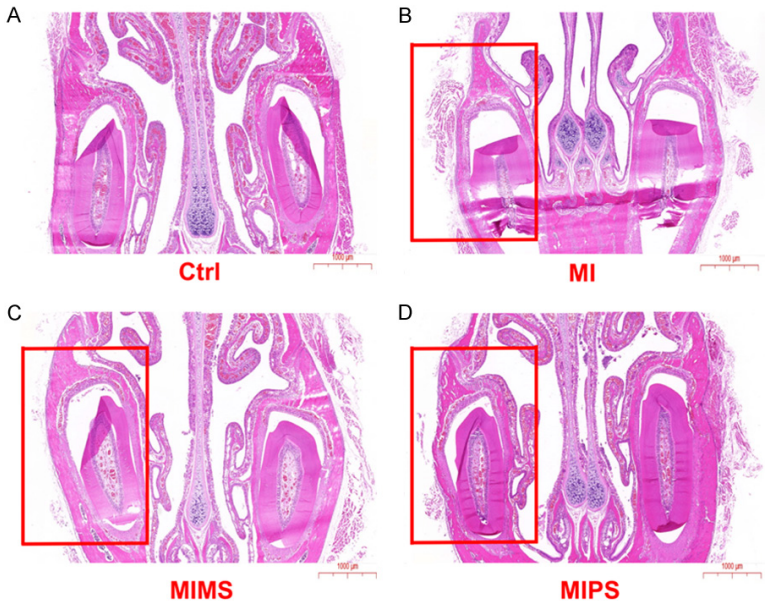

Figure 8. H&E staining photographs of rat premaxillary on coronal section. (A) Ctrl group: The periosteum and musculature were intact, (B) MI group: The periosteum was intact and the muscles still attached to the premaxilla on both sides, (C) MIMS group: The periosteum is continuous, while the muscles are detached on the affected side, (D) MIPS group: The continuity of periosteum is damaged.

growth of the skull, especially in areas under direct masticatory muscle influence, as the sites of masseter muscle attachment. Mavropoulos et al. [17] investigated the effect of masticatory function rehabilitation on the morphology and trabecular architecture of the mandibular alveolar bone after cessation of growth in adult rats. Animal experiments have shown that functional improvement of masticatory muscles may influence the morphology of the mandible on the sagittal and vertical plane as well as the internal structure of the mandibular alveolar bone. These studies confirmed that hypofunction and paralysis of the facial muscle led to craniofacial growth and development restriction, and implied the importance of restoring muscle function during the course of clinical treatment.

Similarly, in the clinical observation of the effects of muscle on the maxillary development in patients with cleft lip and palate, it also suggested that the perioral muscles influenced maxillary development, but the results were inconsistent [18-21]. Therefore, we conducted an animal experiment with perioral muscles as a single factor. In our experiment, we evaluated the effect of the perioral muscle continuity on the three-dimensional premaxillary architecture of growing rats by micro-CT [15, 22]. As we know, periosteum is highly vascularized and contains a variety of cells, such as osteoblasts, osteoclasts, mesenchymal stem cells, and various growth factors, which are the key to osteogenesis [23]. In our 3D imaging results, we could see that significant growth restriction occurred on the affected side compared with the unaffected side following a periosteal disruption (**Figure 5**). For further study, we measured premaxillary length ventrally and dorsally and performed comparisons between controls and intra-group to observe the muscle effect on premaxillary development. The cephalometric measurements suggested that premaxillary length on the affected side was significantly shorter than on the unaffected side ventrally in the three surgical groups and dorsally in the MIPS group (**Table 2**; **Figure 7**). Simultaneously, significant differences were present in intra-group comparisons, except for the comparison between MI and MIMS groups (**Table 3**; **Figure 7**). Combined with the above results, we could conclude that perioral muscle integrity was the main factor affecting premaxillary development when the periosteum was intact. Previous research focused more on the development of mandible after injection BTX-A into the masseter [5, 8] and significant differences were manifested in certain heights and widths.

With intact musculature, growth stimulation can be transmitted to the sutures and maxillary periosteum and positively influence the development of the midface [24]. The muscles at the ectopic attachment point cause dislocation of the muscle fibers, not only deforming the bony surface but also changing the perioral muscle tension [25]. In our experiment, the H&E-stained tissue sections described pathological changes of the premaxilla on the affected side. When the periosteum was intact in MI and MIMS groups, we could observe muscle discon-

tinuity and no conspicuous bony defects in the premaxilla. However, the muscle was shredded after being decalcified in the MIMS group (**Figure 8**). Combined with 3D reconstruction images and 2D coronal sections, bone deposition decreased and a morphologic change was induced, which was only altered primarily at attachment sites of the orbicularis oculi muscle overlying the muscle group (**Figures 5**, **6**). We could observe the superimposition effect of bone morphology changes in the MIMS group. In the MIMS group, premaxillary width was significantly shorter on the affected side than the unaffected side, corresponding to the attachment area of the stripped orbicularis oculi muscle (**Table 1**; **Figure 7**). Our findings suggested that muscle tension affected bone development through muscle attachment points and played a role in plasticity. Muscles exert a contraction force on the periosteum. Bone deposition occurs when a pulling force is applied to the periosteum [23]. This was not discussed in a previous article in which measurements and discussions focused on the volumes of the maxilla or hard tibia [26].

In the reconstruction of cleft lip and palate, many plastic surgeons are also concerned about the effect of muscle reconstruction on maxillary development. A cleft lip involves continuous rupture of the perioral muscle, muscle atrophy, and dislocation [27]. The same pathologic changes could be observed in our H&E-stained sections. In clinical research, Capelozza et al. [28] measured the affected length of the maxilla and found the measurements were shorter in adult patients with unilateral cleft lip and palate than normal patients, which was consistent with our experimental results in three surgical groups. An upward pull on the cleft segment may affect the growth and shaping of the affected side [19]. In our experiment, the average premaxillary widths on the affected sides were longer than on the unaffected sides in the MI group though there was no significant difference. This trend might be due to the discontinuity of the orbicularis oris muscle, which provided stability to the zygomatic arch. When the muscle attachment points in the MIMS group are misplaced, the upward pull cannot act on the periosteum. The average premaxillary widths on the affected sides were shorter than on unaffected sides in the MIMS group. However, the existence of cleft lip in the clinic is mostly accompanied by cleft alveolus or palate [29]. When studying the influence of perioral muscles on craniofacial development, it is difficult to rule out the influence of genetics and cleft palate. The research by Bishara et al. [30] showed that the horizontal maxillary length was longer in unoperated patients with bilateral cleft lip and palate, and similar between unilateral cleft lip and alveolus. Our experiment made muscle a single study factor, which further suggested the importance of muscle reconstruction in cleft lip surgery.

We utilized inexpensive, easy-to-feed and easy-to-operate-on rats as our research object. Some limitations of the present study should be mentioned. The sample size, though small, did allow us to observe statistical significance. A larger sample size, however, may have been better able to demonstrate statistical significance with improved power [31]. Second, we still have no way to completely eliminate the effect of scarring on the experimental results during the healing process in rats. Surgical disinsertion of the orbicularis oculi muscle from the premaxilla may not entirely simulate the ectopic attachment of the orbicularis oculi muscle that occurs under natural growth conditions. In our later studies, we will include a cleft repair group to further confirm the effect of the lip muscle on development of the premaxilla.

Conclusion

From this in vivo experiment, it is concluded that complete perioral muscle continuity with intact attachment to premaxilla is a component of the driving force for premaxillary development, suggesting that craniofacial attached muscles affect the skeletal morphology and this needs to be considered during muscle reconstruction.

Acknowledgements

Jia Zhou is supported by the National Natural Science Foundation of China [Grant No.: 82072175, 81601688], the Shanghai Pujiang Program [Grant No.: 2020PJD027], as well as Shanghai Municipal Key Clinical Specialty [SHSLCZDZK 00901].

Disclosure of conflict of interest

None.

Address correspondence to: Drs. Jia Zhou and Jian Wang, Department of Plastic and Reconstructive Surgery, Shanghai Ninth People's Hospital, Shanghai Jiao Tong University, School of Medicine, No. 639 Zhizaoju Road, Shanghai 200011, China. Tel: +86-021-63135124; Fax: +86-021-63085679; E-mail: joyjb@163.com (JZ); drwangjian@126.com (JW); Dr. Jing Wang, Department of Otorhinolaryngology Head and Neck Surgery, Shanghai Children's Hospital, Shanghai Jiao Tong University, 355 Luding Road, Shanghai 200011, China. Tel: +86-021-62474880; E-mail: wangjing80s@163.com

References

[1] Kim E, Wu F, Wu X and Choo HJ. Generation of craniofacial myogenic progenitor cells from human induced pluripotent stem cells for skeletal muscle tissue regeneration. Biomaterials 2020; 248: 119995.

[2] Hulsey CD, Garcia de Leon FJ and Rodiles-Hernandez R. Micro- and macroevolutionary decoupling of cichlid jaws: a test of Liem's key innovation hypothesis. Evolution 2006; 60: 2096-2109.

[3] Conith AJ, Lam DT and Albertson RC. Muscle-induced loading as an important source of variation in craniofacial skeletal shape. Genesis 2019; 57: e23263.

[4] Kono K, Tanikawa C, Murata Y, Yanagita T, Kamioka H and Yamashiro T. Three-dimensional changes in the craniofacial complex associated with soft-diet feeding. Eur J Orthod 2020; 42: 509-516.

[5] Seok H, Kim SG, Kim MK, Jang I and Ahn J. Effect of the masseter muscle injection of botulinum toxin A on the mandibular bone growth of developmental rats. Maxillofac Plast Reconstr Surg 2018; 40: 5.

[6] Pepicelli A, Woods M and Briggs C. The mandibular muscles and their importance in orthodontics: a contemporary review. Am J Orthod Dentofacial Orthop 2005; 128: 774-780.

[7] Rabey KN, Green DJ, Taylor AB, Begun DR, Richmond BG and McFarlin SC. Locomotor activity influences muscle architecture and bone growth but not muscle attachment site morphology. J Hum Evol 2015; 78: 91-102.

[8] Matic DB, Yazdani A, Wells RG, Lee TY and Gan BS. The effects of masseter muscle paralysis on facial bone growth. J Surg Res 2007; 139: 243-252.

[9] Meng T, Shi B, Wang Q, Zheng Q, Wu M, Huang L, Long J, Li S, Wang Y and Li B. A comparative study of maxillary growth following rotation-advancement and triangular flap unilateral cleft lip repairs: an experimental study in rabbits. Ann Plast Surg 2007; 58: 434-440.

[10] Diah E, Lo LJ, Huang CS, Sudjatmiko G, Susanto I and Chen YR. Maxillary growth of adult patients with unoperated cleft: answers to the debates. J Plast Reconstr Aesthet Surg 2007; 60: 407-413.

[11] Bichara LM, Araujo RC, Flores-Mir C and Normando D. Impact of primary palatoplasty on the maxillomandibular sagittal relationship in patients with unilateral cleft lip and palate: a systematic review and meta-analysis. Int J Oral Maxillofac Surg 2015; 44: 50-56.

[12] Lambrecht JT, Kreusch T and Schulz L. Position, shape, and dimension of the maxilla in unoperated cleft lip and palate patients: review of the literature. Clin Anat 2000; 13: 121-133.

[13] Moss ML and Rankow RM. The role of the functional matrix in mandibular growth. Angle Orthod 1968; 38: 95-103.

[14] Choi J, Park SW, Kwon GY, Kim SH, Hur JA, Baek SH, Kim JC, Choi TH and Kim S. Influence of congenital facial nerve palsy on craniofacial growth in craniofacial microsomia. J Plast Reconstr Aesthet Surg 2014; 67: 1488-1495.

[15] Bresin A, Kiliaridis S and Strid KG. Effect of masticatory function on the internal bone structure in the mandible of the growing rat. Eur J Oral Sci 1999; 107: 35-44.

[16] Katsaros C, Berg R and Kiliaridis S. Influence of masticatory muscle function on transverse skull dimensions in the growing rat. J Orofac Orthop 2002; 63: 5-13.

[17] Mavropoulos A, Odman A, Ammann P and Kiliaridis S. Rehabilitation of masticatory function improves the alveolar bone architecture of the mandible in adult rats. Bone 2010; 47: 687-692.

[18] Mars M and Houston WJ. A preliminary study of facial growth and morphology in unoperated male unilateral cleft lip and palate subjects over 13 years of age. Cleft Palate J 1990; 27: 7-10.

[19] Shetye PR. Facial growth of adults with unoperated clefts. Clin Plast Surg 2004; 31: 361-371.

[20] Liao YF and Mars M. Long-term effects of clefts on craniofacial morphology in patients with unilateral cleft lip and palate. Cleft Palate Craniofac J 2005; 42: 601-609.

[21] Isiekwe MC and Sowemimo GO. Cephalometric findings in a normal Nigerian population sample and adult Nigerians with unrepaired clefts. Cleft Palate J 1984; 21: 323-328.

[22] Mavropoulos A, Kiliaridis S, Bresin A and Ammann P. Effect of different masticatory functional and mechanical demands on the structural adaptation of the mandibular alveolar bone in young growing rats. Bone 2004; 35: 191-197.

[23] Dorfl J. Migration of tendinous insertions. II. Experimental modifications. J Anat 1980; 131: 229-237.

[24] Breitsprecher L, Fanghanel J, Metelmann HR, Mlynski G, Wurfel F, Freise K and Knape U. The influence of the muscles of facial expression on the development of the midface and the nose in cleft lip and palate patients. A reflection of functional anatomy, facial esthetics and physiology of the nose. Ann Anat 1999; 181: 19-25.
[25] Sun M, Wang YQ, Li HD, Wu D, Yin NB and Song T. "Three subunit" classification of lesser-form cleft lip and muscle analysis and reconstruction of these subunits based on the microanatomic structures of muscles in the normal upper lip. J Craniofac Surg 2019; 30: 1790-1793.
[26] Ye B, Ruan C, Hu J, Yang Y, Thomas J and Zhang G. A comparative study on the measurements of palatal shelf area and gradient for adult patients with unoperated cleft palate. Cleft Palate Craniofac J 2012; 49: 561-565.
[27] Kim EK, Khang SK, Lee TJ and Kim TG. Clinical features of the microform cleft lip and the ultrastructural characteristics of the orbicularis oris muscle. Cleft Palate Craniofac J 2010; 47: 297-302.
[28] Capelozza Junior L, Taniguchi SM and da Silva Junior OG. Craniofacial morphology of adult unoperated complete unilateral cleft lip and palate patients. Cleft Palate Craniofac J 1993; 30: 376-381.
[29] Mossey PA, Shaw WC, Munger RG, Murray JC, Murthy J and Little J. Global oral health inequalities: challenges in the prevention and management of orofacial clefts and potential solutions. Adv Dent Res 2011; 23: 247-258.
[30] Bishara SE, de Arrendondo RS, Vales HP and Jakobsen JR. Dentofacial relationships in persons with unoperated clefts: comparisons between three cleft types. Am J Orthod 1985; 87: 481-507.
[31] Antonarakis GS, Tompson BD and Fisher DM. Preoperative cleft lip measurements and maxillary growth in patients with unilateral cleft lip and palate. Cleft Palate Craniofac J 2016; 53: e198-e207.